Available online at www.sciencedirect.com
ScienceDirect
Trans. Nonferrous Met. Soc. China 32(2022) 2080−2090
Transactions of Nonferrous Metals Society of China
www.tnmsc.cn

Electro-enhanced adsorption of As(V) by activated carbon in three-dimensional electrode reactor

Yong-jian LUO[1], Yun-yan WANG[1,2], Hui XU[1], Jia-li DU[1], Ming-fei ZHU[1], Li-min ZHANG[1], Zhu-mei SUN[1,3]

1. School of Metallurgy and Environment, Central South University, Changsha 410083, China;
2. Chinese National Engineering Research Center for Control & Treatment of Heavy Metal Pollution, Central South University, Changsha 410083, China;
3. School of Environment and Safety Engineering, North University of China, Taiyuan 030051, China

Received 28 January 2021; accepted 6 April 2022

Abstract: This study focused on As(V) removal by electrosorption in a self-made three-dimensional electrode reactor, in which granular activated carbon (GAC) was used as the particle electrode. Under the optimal conditions, the removal efficiency of As(V) was 84%, and its residual concentration in solution was 0.08 mg/L. From kinetic investigation, the rate determining steps of the entire process may involve more than two processes: membrane diffusion, material diffusion and physical/chemical adsorption processes. During the desorption process, As(V) can be desorbed from GAC, and the GAC was able to electro-adsorb As(V) again after desorption, which means that the electrode has good cycling performance.

Key words: arsenic removal; activated carbon; electrosorption; three-dimensional electrode reactor

1 Introduction

Nowadays, arsenic contamination in water has received widespread attention due to numerous health problems caused by lifetime exposure to arsenic in many regions of the world [1−3]. In order to increase public awareness of the toxicity of arsenic and minimize the risk of arsenic in water, the International Agency for Research on Cancer (IARC) has recognized both arsenic and arsenic compounds as Class I carcinogens. The World Health Organization (WHO) recommends that the maximum contaminant level of arsenic in drinking water is 0.01 mg/L [4,5].

With the rapid development of society, mining, smelting and chemical industries have got vigorously developed. Meanwhile, excessive metallurgy poses a serious threat to the environment, like the discharge of arsenic-containing wastewater. Although it has been treated properly to satisfy the emission standards (0.5 mg/L), the arsenic concentration in the effluent is still very high, resulting in a large amount of arsenic entering the environment. In addition, the threshold for arsenic in surface water is only 0.1 mg/L according to relevant standards. Therefore, methods to further reduce the emissions of arsenic are essential.

A number of technologies have been developed to remove arsenic from solutions with low concentration, for instance, precipitation [6], adsorption [7], reverse osmosis [8], ion exchange [9], and bio-remediation [10]. Traditional physical-chemical processes are relatively expensive or ineffective, while conventional bio-treatments are not effective. Among them, adsorption has been recognized as an effective method to remove arsenic from solution. Due to its high surface area

Corresponding author: Zhu-mei SUN, Tel: +86-731-89875182, E-mail: sunzhumei41@163.com
DOI: 10.1016/S1003-6326(22)65932-6

(>300 m^2/g), wide range of pore volume, great conductivity and chemical stability, granular activated carbon (GAC) has been widely utilized as a common carrier for adsorbent [11]. However, the limited adsorption capacity of GAC and the inability of full regeneration restrict its application for wastewater treatment [12]. Hence, it is necessary to find a method that can improve the adsorption capacity of GAC while achieving efficient and economic regeneration for practical applications.

Capacitive deionization (CDI) is an emerging technology that enhances the adsorption capacity and adsorption efficiency of electrode materials by applying an external electric field [13]. What's more, it has the characteristics of low operating cost and low potential secondary pollution [14]. Some reports [15,16] have confirmed that GAC as the electrode can remove arsenic effectively. However, all the above studies were based on a groundwater concentration (lower than 0.1 mg/L), and the treatment capacity was small (less than 200 mL). Thus, on behalf of effectively solving the limitations of CDI, the concept of three-dimensional (3D) electrodes was proposed [17]. The 3D electrochemical process was established and developed from the traditional two-dimensional (2D) electrochemical process. In comparison with 2D electrochemical process, the introduction of particle electrodes brought about higher specific surface area and shorter distance of mass transfer [18]. At present, 3D electrode process is mainly used in the field of electro-catalytic oxidation [19], although it has many functions, like electrosorption and electrocoagulation [20,21], which make it more promising for environmental application.

In this study, an electrochemical method of As(V) removal and regeneration of GAC in a 3D electrode reactor was developed. It aimed at achieving deep treatment of As(V) in solution, and finally reduced As(V) pollution to the environment. During the experiments, the effect of some parameters on As(V) removal efficiency was investigated. Afterwards, kinetic models of pseudo-first-order, pseudo-second-order, and intra-particle diffusion were used to analyze the electrosorption process. Ultimately, a novel combined process of electrosorption−desorption was developed for As(V) removal and recycling.

2 Experimental

2.1 Materials

The GAC made from coconut shell was obtained from Ningbo Youshi Carbon Factory Co., Ltd., China. Titanium mesh with purity of 99% was purchased from Cangzhou Kangwei Metal Products Co., Ltd., China. Sodium arsenate tribasic dodecahydrate ($Na_3AsO_4·12H_2O$) used to prepare As(V) solution was analytically pure.

2.2 Preparation of electrodes

The GAC with particle size larger than 0.6 mm was selected. The GAC was put into deionized water and stirred. 0.5 mol/L concentrated nitric acid was added dropwise for acidification until the pH was stabilized at 3 for 0.5 h. Eventually, the acidified GAC was washed with deionized water until pH was close to be neutral, and dried in an oven at 105 °C.

2.3 Experimental equipment

The sketch of the self-made 3D electrode reactor was shown in Fig. 1. The reactor was made of PVC plastic, and the dimensions of the reactor were 10 cm × 4 cm × 5 cm. The anode and cathode were both made from titanium mesh with dimensions of 5 cm × 3 cm. The distance between the anode and the cathode can be adjusted. The cathode electrode and the particle electrode were separated by gauze. The reactor was powered by a DC source. The peristaltic pump was used to draw

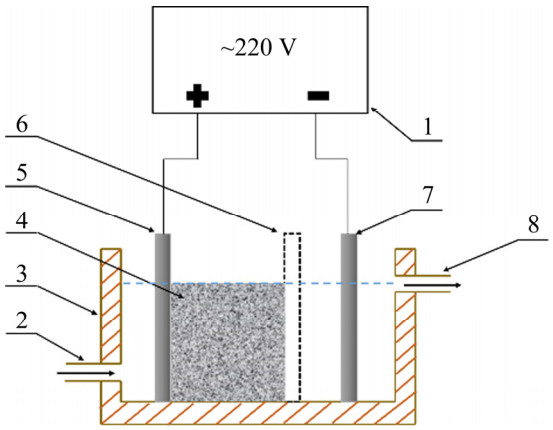

Fig. 1 Sketch of 3D electrode reactor: 1—DC power; 2—Inlet; 3—Reaction tank; 4—Particle electrodes; 5—Titanium mesh anode; 6—Gauze; 7—Titanium mesh cathode; 8—Outlet

the solution into the reactor, and the solution was eventually circulated at a flow rate of no more than 125 mL/min (the speed of pump was 50 r/min).

2.4 Adsorption experiment

The experiment was carried out by placing 15 g of pre-treated GAC in solution to adsorb As(V) at room temperature. The As(V) initial concentration was 0.5 mg/L. The experimental parameters, such as pH, applied voltage, and flow rate, were optimized through single-factor experiments. After a period, GAC reached equilibrium.

2.5 Electrosorption experiment

The GAC pretreated by adsorption was placed in the 3D electrode reactor, and 800 mL of 0.5 mg/L As(V) solution was subjected to electrosorption under a certain voltage until the pH of the solution no longer changed. The changes of solution pH were monitored by a pH meter (PHS−2F).

2.6 Measurements

The surface morphology and pore-size distribution of GAC were characterized by scanning electron microscopy (SEM, JSM−6360LV) and Brunauer−Emmett−Teller (BET, ASPS 2460), respectively. The As(V) concentrations were determined by inductively coupled plasma-optical emission spectrometer (ICP-OES, ICAP7400 Radial).

3 Results and discussion

3.1 Characterization of particle electrode

SEM images of the GAC were presented in Fig. 2. It was found that the GAC was in an irregular granular form. Macro-pores, meso-pores and micro-pores on the surface were interlaced, and the average pore diameter was 0.8237 nm. This indicated that the GAC had high porosity. The specific surface area of GAC was detected by the BET test to be 403.3833 m^2/g. The N_2 adsorption−desorption isotherm in Fig. 3 revealed that the selected GAC had a great pore structure. To sum up, the GAC could be used as a good adsorption material.

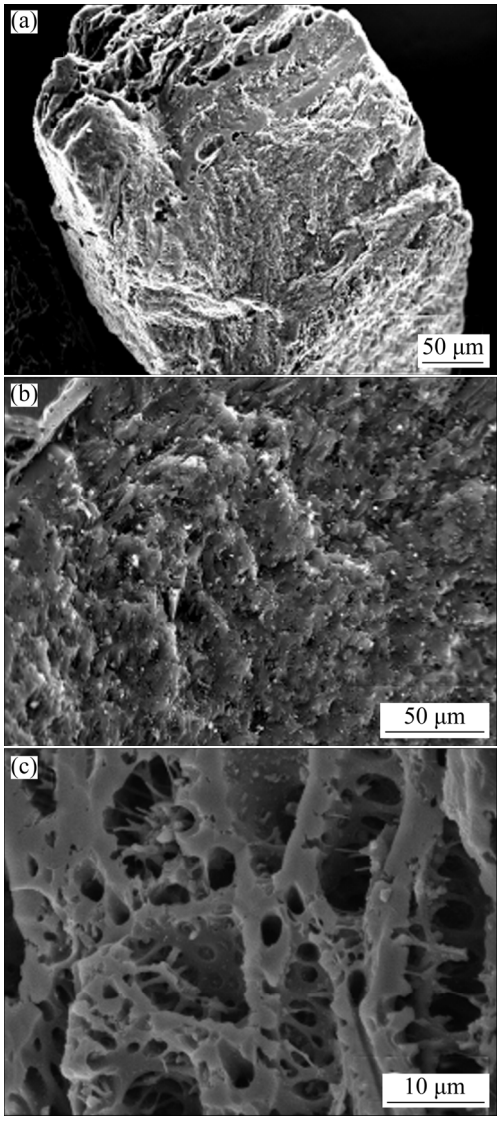

Fig. 2 SEM images of GAC

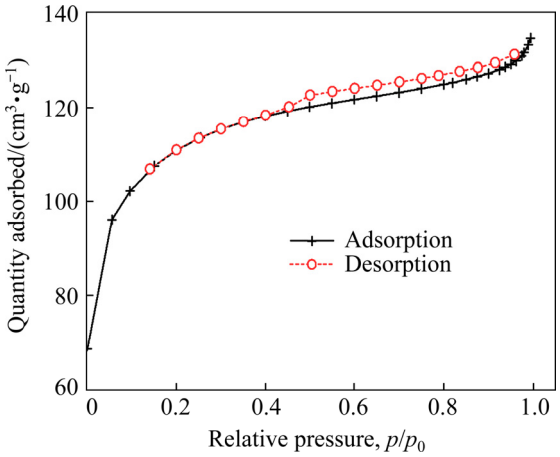

Fig. 3 N_2 adsorption−desorption isotherms of GAC

3.2 Adsorption of As(V) by GAC

In this experiment, an Erlenmeyer flask containing 15 g of GAC and 200 mL of As(V) solution (pH 3) was placed in an oscillator (TS−100B) to perform vibrational adsorption, at a volatile rate of 25 r/min. As shown in Fig. 4, the

adsorption experiment reached equilibrium at 12 h, and the concentration of As(V) was 0.46 mg/L. The result indicated that GAC had a limited ability to remove As(V) at this concentration by adsorption. This phenomenon might be ascribed to the following aspects: (1) the carbon materials are not effective against arsenic adsorption [22]; (2) the concentration of As(V) in the solution is too low to fully contact with the GAC, and then results in poor adsorption effect [23].

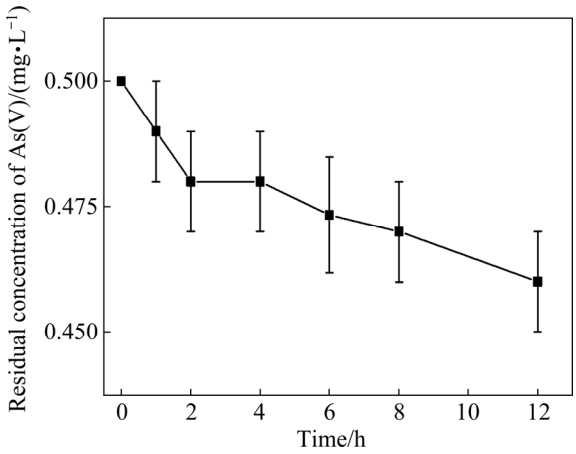

Fig. 4 Residual concentration of As(V) in adsorption experiment by GAC

3.3 Electrosorption of As(V) by GAC

3.3.1 Effect of electrosorption time

To determine the effect of the electrosorption time, the experiment was conducted under the conditions that the pH of As(V) solution was 3, the flow rate was 38 mL/min, and the voltage was 1.2 V. The thickness of packed bed of the pretreated GAC was 1 cm (GAC dosage was 15 g). The residual As(V) concentration in the effluent was shown in Fig. 5. The curve of the residual As(V) concentration showed a rapid decline to a slow one, and finally reached an equilibrium state at 12 h, where the residual As(V) equilibrium concentration of the solution is 0.28 mg/L.

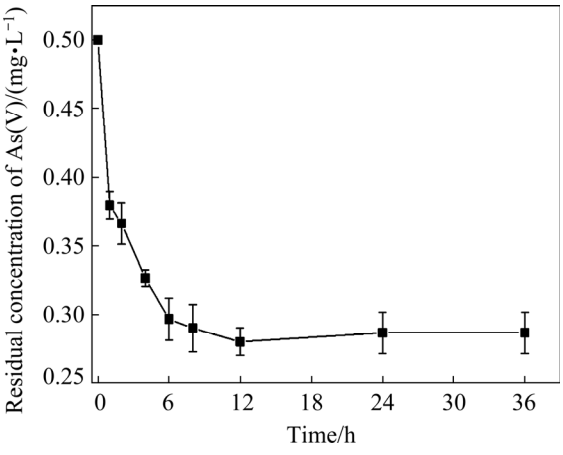

Fig. 5 Effect of time on electrosorption of As(V)

According to some reports [24,25], hydraulic retention time was the corresponding important parameter for the continuous flow electrochemical reactor. Too short treatment time will reduce the removal efficiency, while prolonging the treatment time will increase the operating cost. Thus, the optimal adsorption time was 12 h.

3.3.2 Effect of thickness of packed bed

The experiments were performed at different thicknesses (1, 2, 3, and 4 cm) of the packed bed, where the initial pH of solutions was 3 and the applied voltage was 1.2 V. The effect of thickness of packed bed on the removal efficiency of As(V) was presented in Fig. 6. As the thickness increased, the removal efficiency became better gradually. The electrosorption capacity was not significantly improved while the residual As(V) concentration was 0.27 mg/L (3 cm) and 0.25 mg/L (4 cm), respectively. As a result, the thickness of GAC packed bed of 3 cm was sufficient for As(V) removal. This can be concluded that the large filling thickness hindered the mass transfer of arsenic in the solution, resulting in insufficient contact between GAC and As(V), and then affects its electrosorption performance. From the perspective of cost saving, the thickness of 3 cm was preferable.

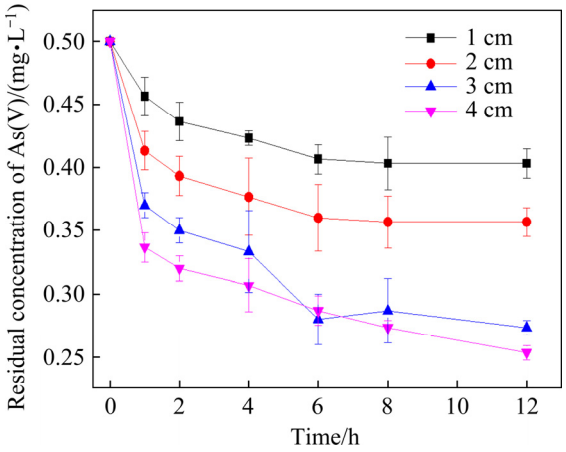

Fig. 6 Effect of thickness of packed bed on electrosorption of As(V)

3.3.3 Effect of pH

It is known that pH has a strong influence on the arsenic species, and the arsenic species makes a great impact of the electrosorption efficiency, so pH

is the key factor affecting the efficiency of arsenic removal. To get a deep insight into the electrosorption process under different pH conditions, the experiment was conducted under the conditions of a packed bed thickness of 3 cm and a voltage of 1.2 V. The results were shown in Fig. 7.

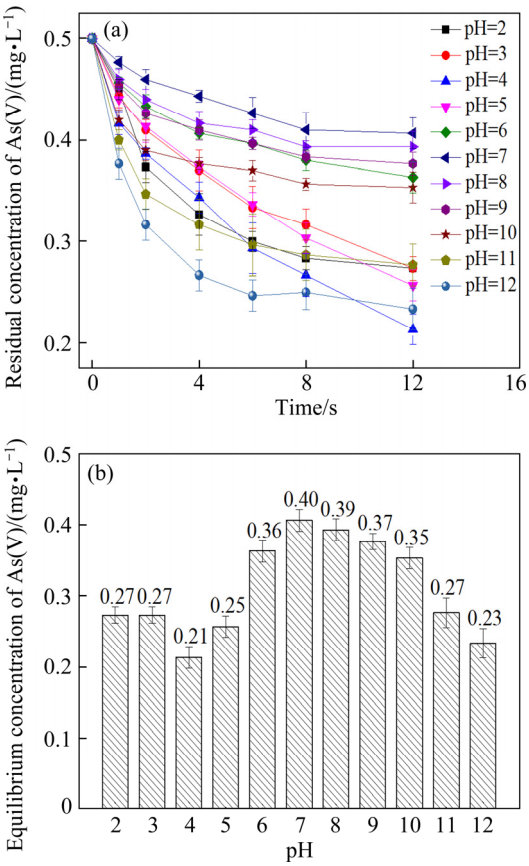

Fig. 7 Effect of pH on electrosorption of As(V): (a) Residual concentration of As(V); (b) Equilibrium concentration of As(V)

The residual As(V) concentrations at the selected pH (2−12) were shown in Fig. 7(a). It can be found that As(V) concentrations decreased gradually over time, but they did not change regularly with pH increasing or decreasing. Since adsorption relies on the strength of binding between sorbents' surface sites to the certain species and the predominant species when multiple species coexist in the polluted water, strong binding species dominate the surface binding sites and considerably decrease the adsorption of weak binding species [23]. According to Fig. 7(b), the As(V) removal efficiencies were low when pH was between 6 and 10. A better removal effect was obtained when pH was 2, 3, 4, 5, 11, and 12, and correspondingly, the residual concentrations were 0.27, 0.27, 0.21, 0.25, 0.27, and 0.23 mg/L, respectively. The best removal efficiency was obtained when the pH was 4. At the same time, the residual concentration at pH of 12 was very close to that at 4, but was still slightly higher. Additionally, this might be attributed to the dramatically increased amount of OH^- in the solution, which rendered it more competitive than any other ions in an alkaline environment, although arsenic was more negatively charged in the solution at pH of 12 ($HAsO_4^{2-}$, AsO_4^{3-}) than at pH of 4 ($H_2AsO_4^-$) according to φ−pH diagram of arsenite and arsenate [26].

3.3.4 Effect of applied voltage

The applied voltage is one of the most significant variable parameters in electrochemical processes since it promotes electrosorption via the polarization of particle electrode to form microelectrodes. The results were given in Fig. 8. In the voltage range of 0−2.4 V, the residual As(V) concentration gradually decreased with an increase of the applied voltage. The equilibrium As(V) concentration was 0.12 mg/L while the applied voltage was 2.4 V.

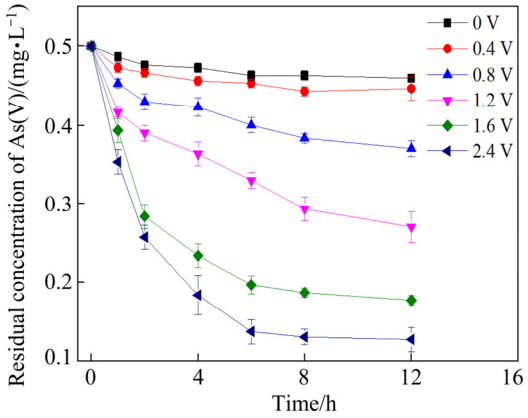

Fig. 8 Effect of applied voltage on electrosorption of As(V)

This result could be explicated that the electric field strength/current density increased with increasing voltage, which in turn facilitated the migration and accumulation of arsenic to the anode, and finally increased the removal performance [27]. Although the treatment performance was enhanced with the increase of the applied voltage, the energy consumption was accordingly increased. Generally, the optimal applied voltage was 2.4 V.

3.3.5 Effect of flow rate

The results of the effect of flow rate on the

electrosorption of As(V) were shown in Fig. 9. The faster the flow rate is, the lower the residual As(V) concentration at each sampling time is. It can be interpreted that the contact between GAC and As(V) was enhanced while the mass transfer increased, and then the removal efficiency was improved [28]. When the adsorption process attained equilibrium state, residual concentrations of As(V) at flow rates of 88 and 125 mL/min were 0.19 and 0.18 mg/L, respectively, and the removal efficiencies were much higher. This phenomenon might be ascribed to the fact that the excessive flow rate produced less retention time, resulting in the inadequate contact with GAC, which weakened the removal performance. So, there was no significant difference in their removal efficiency when the flow rates were 88 and 125 mL/min, respectively. Above all, the optimal flow rate in this system was 88 mL/min.

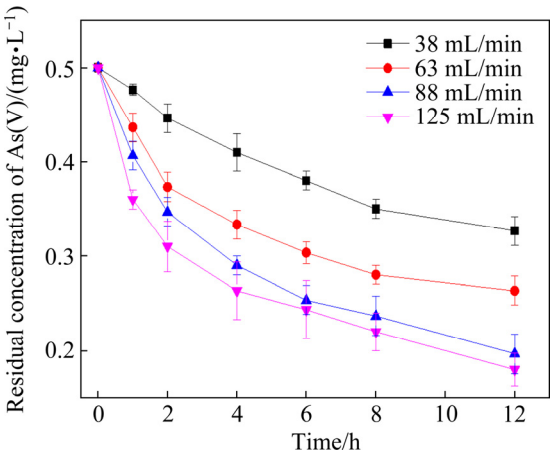

Fig. 9 Effect of flow rate on electrosorption of As(V)

3.3.6 Results under optimal experimental conditions

As evidenced, the electro-enhanced adsorption in the 3D electrode reactor showed a great performance. The optimal experimental parameters were systematically summarized as follows: the time was 12 h, the thickness of packed bed was 3 cm, the voltage was 2.4 V, the pH was 4, and the flow rate was 88 mL/min. Accordingly, the removal efficiency was shown in Fig. 10. The residual As(V) concentration was 0.08 mg/L, which was lower than the threshold (0.1 mg/L) in surface water in China (GB3838—2002). The deep treatment of arsenic was achieved. This meant that As(V) removal could be improved by utilizing a 3D electrode reactor, that is, the electric field can increase the adsorption capacity of the GAC.

In Fig. 11, SEM and EDS images of electrode revealed that there was As(V) on the surface of

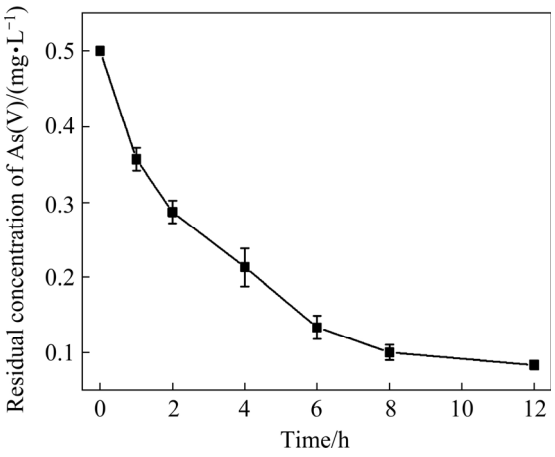

Fig. 10 Residual As(V) concentration under optimal experiment conditions

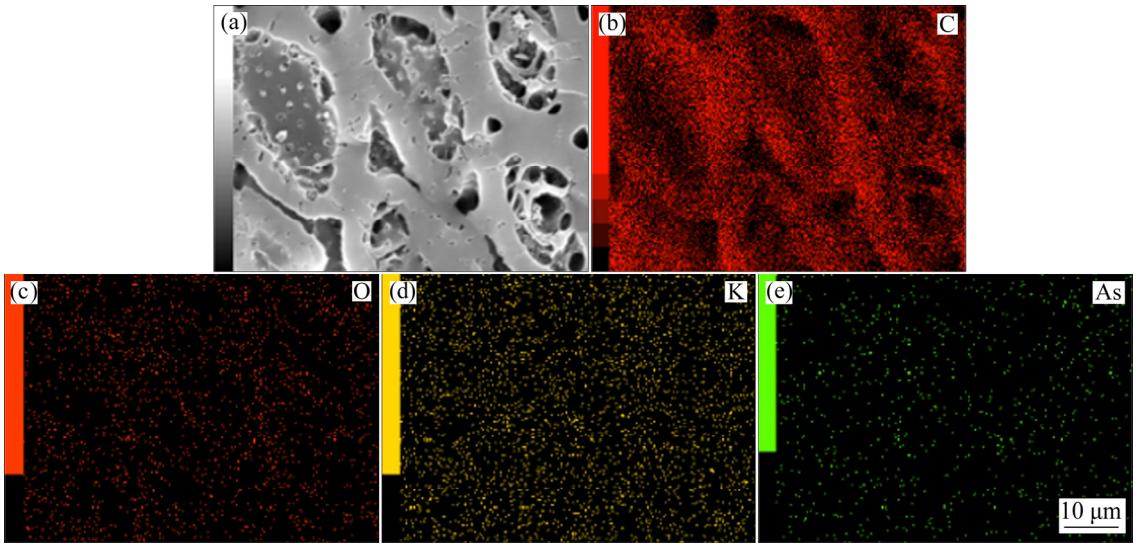

Fig. 11 SEM image (a) and element distribution (b−e) of GAC electrode after As(V) electrosorption

GAC. Therefore, it can be speculated that As(V) migrated to the anode under the action of electric field, and was finally adsorbed in the pores of the electrode. The electric-double layer was formed on the electrode surface, which was presented in Fig. 12. From Fig. 12, it can be seen that there were electrosorption and physical adsorption during the whole process.

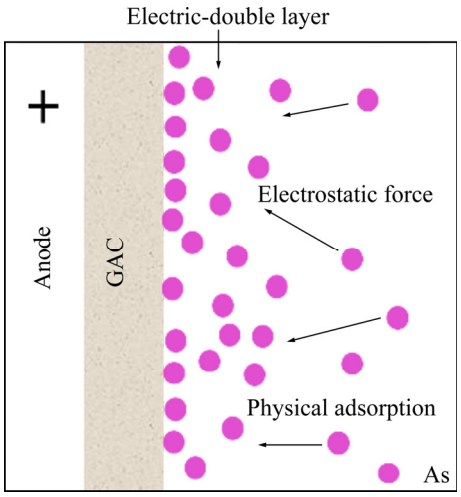

Fig. 12 Mechanism of As(V) removal by electrosorption

3.3.7 Effect of influent concentration fluctuation

Arsenic concentration in wastewater may fluctuate in the actual production processes. Therefore, it is necessary to determine the influence of arsenic concentration fluctuation on the quality of treated effluent by electrosorption. In order to investigate this factor, the experiments were carried out under optimal conditions, but the initial As(V) concentrations were 0.1, 0.5, 0.6, 0.7, 0.8, 0.9, and 1.0 mg/L, respectively. The results were presented in Fig. 13.

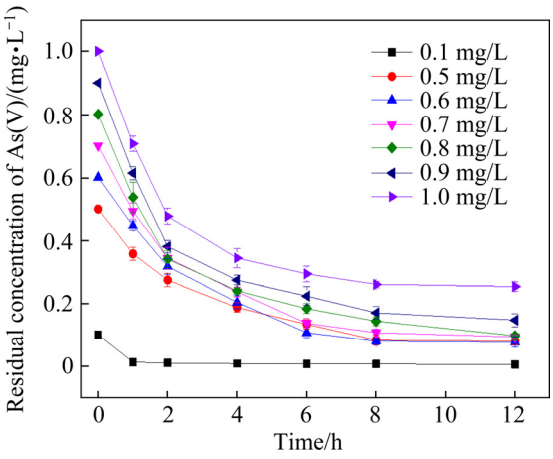

Fig. 13 Effect of influent concentration fluctuation on electrosorption of As(V)

The results showed that the outlet As(V) concentration could reach the limits specified in the environmental quality standards for surface water (GB3838—2002) in China when the initial As(V) concentration of the inlet water was lower than 0.8 mg/L. And, the outlet As(V) concentration was 0.1 mg/L when the initial As(V) concentration was 0.8 mg/L. This meant that this technique is resistant to fluctuations in concentrations. In general, the initial As(V) concentration had a great influence on the removal efficiency by electrosorption in the 3D electrode reactor, and it was still necessary to optimize the 3D electrode electrosorption technology.

3.4 Adsorption kinetics

Adsorption kinetics can provide information about the adsorption mechanism and describe the interaction according to appropriate mathematical models (Eqs. (1)−(3)) [29−31]:

$$\ln(q_e - q_t) = \ln q_e - k_1 t \tag{1}$$

$$\frac{t}{q_t} = \frac{1}{k_2 q_e^2} + \frac{t}{q_e} \tag{2}$$

$$q_t = k_3 t^{0.5} + c \tag{3}$$

where k_1, k_2 and k_3 represent rate constants of the pseudo-first-order adsorption (min^{-1}), the pseudo-second-order adsorption ($g \cdot mg^{-1} \cdot min^{-1}$), and intra-particle diffusion ($mg \cdot g^{-1} \cdot min^{-0.5}$), respectively; q_e ($mg \cdot g^{-1}$) and q_t ($mg \cdot g^{-1}$) are the capacities of adsorbed arsenic ions at equilibrium and time t, respectively; c stands for the intercept depicting the boundary layer effect. The data of adsorption kinetic models were shown in Fig. 14 and Table 1.

It can be concluded that the pseudo-second-order kinetic coefficient (R^2=0.9923) was superior to the pseudo-first-order kinetic coefficient (R^2= 0.9708). So, electrosorption kinetics on the GAC was regarded as pseudo-second-order rather than pseudo-first-order kinetic model, which verified that the electrosorption process obeyed the pseudo-second-order kinetic model when the initial concentration of solution was not too high. It also validated that the electrodes (adsorption materials) were easy to reach adsorption saturation state, which accorded with the general rule of carbon materials [32].

The main factors limiting adsorption rate were the liquid film diffusion process and the internal diffusion process during the adsorption process [33].

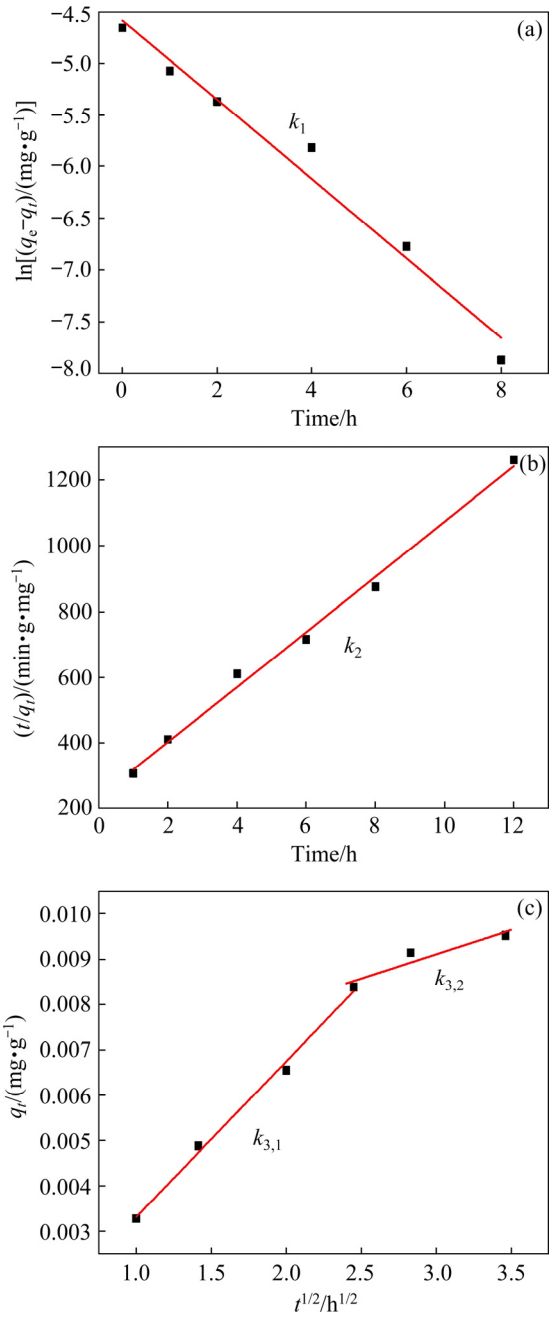

Fig. 14 Adsorption kinetics models of As(V) adsorption: (a) Pseudo-first-order; (b) Pseudo-second-order; (c) Intra-particle diffusion

Table 1 Electrosorption parameters of pseudo-first-order, pseudo-second-order kinetics and intra-particle diffusion

Kinetic model	Parameter	R^2
Pseudo-first-order	k_1=0.0304 min^{-1}	0.9708
Pseudo-second-order	k_2=0.0352 $g\cdot mg^{-1}\cdot min^{-1}$	0.9923
Intra-particle diffusion	$K_{3,1}$=0.0026 $mg\cdot g^{-1}\cdot min^{-0.5}$	0.9313
	$K_{3,2}$=0.0010 $mg\cdot g^{-1}\cdot min^{-0.5}$	0.9146

Therefore, we adopted the intra-particle diffusion model to fit the adsorption process in order to better analyze the adsorption process. According to Fig. 14(c), the intra-particle diffusion model was divided into two sections representing the membrane diffusion process of arsenic from the solution to the surface of electrode materials, and the diffusion process of arsenic from the surface of electrode materials to internal pores, respectively. These two diffusion stages were illustrated in Fig. 15. The plot of q_t versus $t^{1/2}$ should be a straight line passing through the origin of coordinates, and c=0 in Eq. (3), if the intra-particle diffusion was the rate determining step of the entire adsorption process. In fact, the straight line with the slope of 0.0010 in the second stage implied that the intra-particle diffusion process was not the only rate determining step. Therefore, in the process of removing arsenic by electrosorption, the rate determining step may involve more than two processes: membrane diffusion, intra-particle diffusion and physical/chemical adsorption processes [34].

3.5 Recycling of electrode

To examine the regeneration of the GAC electrodes, electrosorption−desorption experiments were conducted with 0.5 mg/L As(V) solution by repeating the charge−discharge process three times in the 3D reactor. The results were shown in Fig. 16.

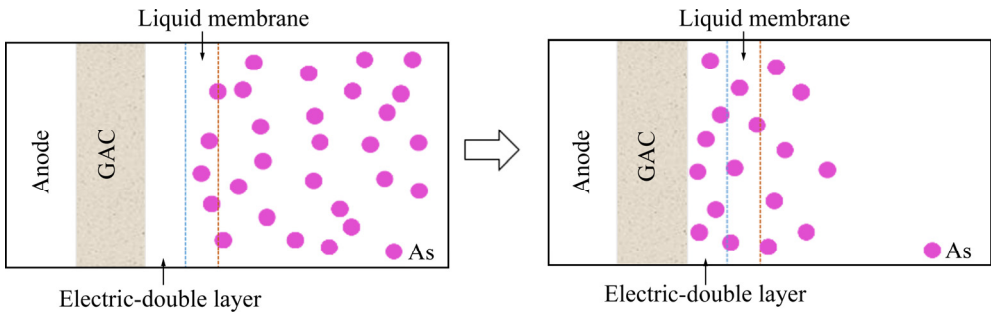

Fig. 15 Two diffusion stages of intra-particle diffusion model in As(V) adsorption process

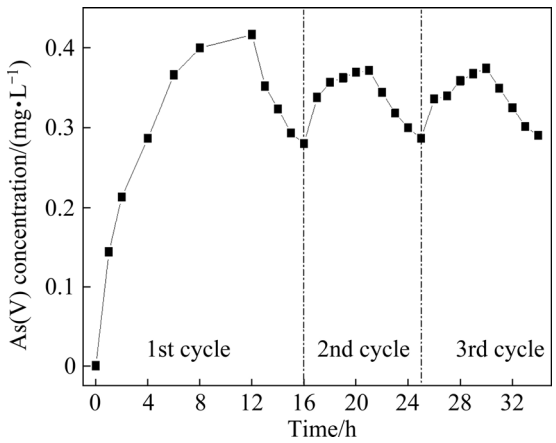

Fig. 16 Electrosorption and desorption cycle regeneration of electrode

For each charge−discharge cycle, the reactor was charged at 2.4 V for 5 h and then discharged at −2.4 V for 4 h, except for the first cycle which was charged for 12 h.

Figure 16 illustrated that the desorption of arsenic was feasible, and the GAC can electro-adsorb As(V) again after desorption. This phenomenon can be explained by the fact that arsenic transfer was driven by the electric field forces, and arsenic was stored at electrode interfaces during the electrosorption stage. Subsequently, arsenic was released from electrode with the electric field disappearing. After three cycles, the electrodes can still effectively electro-adsorb/desorb As(V), which indicated that the electrodes had good cycle performance and regeneration.

4 Conclusions

(1) Under the optimized conditions, the As(V) removal efficiency reached 84%, that is, the As(V) concentration in effluent was reduced from 0.5 to 0.08 mg/L, which met environmental quality standards for surface water (GB3838—2002) in China.

(2) It was verified that the applied electric field can effectively improve the adsorption capacity of GAC after adsorption pretreatment, and the deep treatment of As(V) by GAC in a 3D electrode reactor was achieved.

(3) It was found from the kinetic investigation of the electrosorption process that the process conforms to the pseudo-second-order kinetic model, and it was concluded that the rate determining steps of the entire process may involve more than two processes: membrane diffusion, material diffusion and physical/chemical adsorption processes.

(4) More importantly, the electrode can be regenerated effectively and had good cycling performance. So, it has a great development prospect.

Acknowledgments

This work was financially supported by the National Natural Science Foundation of China (No. 52004256), the Shanxi Provincial Science Foundation for Youths, China (No. 201901D211212), the Scientific and Technological Innovation Programs of Higher Education Institutions in Shanxi Province, China (No. 2019L0574), the Young Academic Leader of North University of China (No. QX202004), and the Postdoctoral Innovative Talent Support Program of Hunan Province, China (2021RC2010).

References

[1] AHMAD A, BHATTACHARYA P. Environmental arsenic in a changing world [J]. Groundwater for Sustainable Development, 2019, 8: 169−171.

[2] SHANKAR S, SHANKER U, SHIKHA. Arsenic contamination of groundwater: A review of sources, prevalence, health risks, and strategies for mitigation [J]. The Scientific World Journal, 2014, 2014: 179−186.

[3] TCHOUNWOU P B, YEDJOU C G, UDENSI U K, PACURARI M, STEVENS J J, PATLOLLA A K, NOUBISSI F, KUMAR S. State of the science review of the health effects of inorganic arsenic: Perspectives for future research [J]. Environmental Toxicology, 2019, 34: 188−202.

[4] FERLAY J, SOERJOMATARAM I, DIKSHIT R, ESER S, MATHERS C, REBELO M, PARKIN D M, FORMAN D, BRAY F. Cancer incidence and mortality worldwide: Sources, methods and major patterns in GLOBOCAN 2012 [J]. International Journal of Cancer, 2015, 136: 359−386.

[5] ORGANIZATION W H. Guidelines for drinking-water quality [M]. 4th ed. Geneva: World Health Organization, 2017.

[6] HU Bin, YANG Tian-zu, LIU Wei-feng, ZHANG Du-chao, CHEN Lin. Removal of arsenic from acid wastewater via sulfide precipitation and its hydrothermal mineralization stabilization [J]. Transactions of Nonferrous Metals Society of China, 2019, 29: 2411−2421.

[7] VADAHANAMBI S, LEE S H, KIM W J, OH I K. Arsenic removal from contaminated water using three-dimensional graphene-carbon nanotube-iron oxide nanostructures [J]. Environmental Science & Technology, 2013, 47:

10510−10517.

[8] CORROTO C E, IRIEL A, CIRELLI A F, CARRERA A L P. Constructed wetlands as an alternative for arsenic removal from reverse osmosis effluent [J]. Science of the Total Environment, 2019, 691: 1242−1250.

[9] CHEN A S C, WANG L L, SORG T J, LYTLE D A. Removing arsenic and Co-occurring contaminants from drinking water by full-scale ion exchange and point-of-use/ point-of-entry reverse osmosis systems [J]. Water Research, 2020, 172: 115455.

[10] KEPEL B, BODHI W, UMAR F, TALLEI T. Isolation and identification of arsenic-resistant bacteria for possible application in arsenic bioremediation [J]. Pakistan Journal of Biological Sciences, 2020, 23: 63−67.

[11] YIN Yu-wei, ZHOU Ting-ting, LUO Han-jin, GENG Jun-jie, YU Wen-yi, JIANG Zhong-jie. Adsorption of arsenic by activated charcoal coated zirconium−manganese nanocomposite: Performance and mechanism [J]. Colloids and Surfaces A, 2019, 575: 318−328.

[12] GUO Dong-sheng, SHI Qian-tao, HE Bin-bin, YUAN Xiao-ying. Different solvents for the regeneration of the exhausted activated carbon used in the treatment of coking wastewater [J]. Journal of Hazardous Materials, 2011, 186: 1788−1793.

[13] AHMED M A, TEWARI S. Capacitive deionization: Processes, materials and state of the technology [J]. Journal of Electroanalytical Chemistry, 2018, 813: 178−192.

[14] ANDERSON M A, CUDERO A L, PALMA J. Capacitive deionization as an electrochemical means of saving energy and delivering clean water. Comparison to present desalination practices: Will it compete? [J]. Electrochimica Acta, 2010, 55: 3845−3856.

[15] HOYOS S G, FLORES M A, RAMIREZ A I, CALDERON C, RAMIREZ-OROZCO A, NIETO A, SHELP G, SEED LEONARD CEBRIAN M, VERA E. Natural arsenic in ground waters of Latin America [M]. Mexico: Taylor & Francis, 2008: 665−676.

[16] LEE J Y, CHAIMONGKALAYON N, LIM J, HA Y H, MOON S H. Arsenic removal from groundwater using low-cost carbon composite electrodes for capacitive deionization [J]. Water Science and Technology, 2016, 73: 3064−3071.

[17] PAN Gang-wei, JING Xiao-hui, DING Xin-yun, SHEN Yong-jun, MIAO Wu-jian. Synergistic effects of photocatalytic and electrocatalytic oxidation based on a three-dimensional electrode reactor toward degradation of dyes in wastewater [J]. Journal of Alloys and Compounds, 2019, 809: 151749.

[18] MA Bei-bei, CHEN Shui-jiao, HUANG Ye-wei, NIE Zhen-zhen, QIU Xiao-bin, XIE Xiu-qiang, WU Zhen-jun. Electrochemical lithium storage performance of three-dimensional foam-like biocarbon/MoS_2 composites [J]. Transactions of Nonferrous Metals Society of China, 2021, 31: 255−264.

[19] REN Jing, LI Hao-xin, LI Na, SONG You-tao, CHEN Jia-yi, ZHAO Lin. A three-dimensional electrode bioelectro-chemical system for the advanced oxidation of *p*-nitrophenol in an aqueous solution [J]. RSC Advances, 2020, 10: 17163−17170.

[20] FOO K Y, HAMEED B H. A short review of activated carbon assisted electrosorption process: An overview, current stage and future prospects [J]. Journal of Hazardous Materials, 2009, 170: 552−559.

[21] TCHAMANGO S R, NGAYO K W, BELIBI P D, NKOUAM F, NGASSOUM M B. Treatment of a dairy effluent by classical electrocoagulation and indirect electrocoagulation with aluminum electrodes [J]. Separation Science and Technology, 2021, 56: 1128−1139.

[22] DAI Min, ZHANG Man, XIA Ling, LI Yan-mei, LIU Yan-yan, SONG Shao-xian. Combined electrosorption and chemisorption of As(V) in water by using Fe-rGO@AC electrode [J]. ACS Sustainable Chemistry & Engineering, 2017, 5: 6532−6538.

[23] SHAH I, ADNAN R, WAN NGAH W S, MOHAMED N. Iron impregnated activated carbon as an efficient adsorbent for the removal of methylene blue: Regeneration and kinetics studies [J]. PloS One, 2015, 10: e0122603.

[24] HAUCHHUM L, MAHANT P. Carbon dioxide adsorption on zeolites and activated carbon by pressure swing adsorption in a fixed bed [J]. International Journal of Energy and Environmental Engineering, 2014, 5: 349−356.

[25] LV Gui-fen, WU Ding-cai, FU Ruo-wen. Performance of carbon aerogels particle electrodes for the aqueous phase electro-catalytic oxidation of simulated phenol wastewaters [J]. Journal of Hazardous Materials, 2009, 165: 961−966.

[26] DAI M, XIA L, SONG S X, PENG C S, RANGEL MENDEZ J R, CRUZ GAONA R. Electrosorption of As(III) in aqueous solutions with activated carbon as the electrode [J]. Applied Surface Science, 2018, 434: 816−821.

[27] HAN Yan-he, QUAN Xie, CHEN Shuo, WANG Shi-bo, ZHANG Yao-bin. Electrochemical enhancement of adsorption capacity of activated carbon fibers and their surface physicochemical characterizations [J]. Electrochimica Acta, 2007, 52: 3075−3081.

[28] SUN Zhu-mei, CHAI Li-yuan, LIU Ming-shi, SHU Yu-de, LI Qing-zhu, WANG Yun-yan, WANG Qing-wei, QIU Ding-fan. Capacitive deionization of chloride ions by activated carbon using a three-dimensional electrode reactor [J]. Separation and Purification Technology, 2018, 191: 424−432.

[29] JIANG Yan-hong, LI An-yu, DENG Hua, YE Cheng-hui, WU Yu-qing, LINMU Yu-dan, HANG Hao-lin. Characteristics of nitrogen and phosphorus adsorption by Mg-loaded biochar from different feedstocks [J]. Bioresource Technology, 2019, 276: 183−189.

[30] KWAK H W, LEE H, LEE K H. Surface-modified spherical lignin particles with superior Cr(VI) removal efficiency [J]. Chemosphere, 2020, 239: 124733.

[31] MAHMOUD M E, AMIRA M F, SELEIM S M, MOHAMED A K. Amino-decorated magnetic metal-organic framework as a potential novel platform for selective removal of chromium(Vl), cadmium(II) and lead(II) [J].

Journal of Hazardous Materials, 2020, 381: 120979.
[32] AZIZIAN S. Kinetic models of sorption: A theoretical analysis [J]. Journal of Colloid and Interface Science, 2004, 276: 47−52.
[33] HO Y S. Review of second-order models for adsorption systems [J]. Journal of Hazardous Materials, 2006, 136: 681−689.
[34] SCHULTZE-JENA A, BOON M A, de WINTER D A M, BUSSMANN P J T, JANSSEN A E M, van der PADT A. Predicting intraparticle diffusivity as function of stationary phase characteristics in preparative chromatography [J]. Journal of Chromatography A, 2020, 1613: 460688.

三维电极反应器中活性炭电化学强化吸附 As(V)

罗永健[1]，王云燕[1,2]，徐 慧[1]，杜嘉丽[1]，朱明飞[1]，张李敏[1]，孙竹梅[1,3]

1. 中南大学 冶金与环境学院，长沙 410083；
2. 中南大学 国家重金属污染防治工程技术研究中心，长沙 410083；
3. 中北大学 环境与安全工程学院，太原 030051

摘 要：采用自制三维电极反应器对溶液中的 As(V)进行电吸附去除，而粒子电极选用活性炭颗粒(GAC)。在最佳条件下，As(V)的去除率为 84%，溶液中 As(V)的残留浓度为 0.08 mg/L。从动力学研究中得到，整个过程的速率控制步骤可能涉及两个以上的过程：膜扩散、物质扩散和物理/化学吸附过程。在脱附过程中，As(V)可以从 GAC 中解吸出来，且 GAC 在解吸后能再次电吸附 As(V)，这表明该电极具有良好的循环性能。

关键词：除砷；活性炭；电吸附；三维电极反应器

(Edited by Wei-ping CHEN)